Investigation on Hansen Solubility Parameter of caffeine dissolved in different pure solvents

ABSTRACT

Aims: ~~The solubility~~Solubility is a molecular property decisive in the entire process from ~~the~~ drug development and design to the final drug formulation and production, the main objective of this paper is ~~explaining~~ to explainthe effect of the variance in molecular properties and intermolecular interaction on dissolution by Hansen Solubility Parameter (HSP) and KAT-LSER model.
Study design:~~The solubility~~ Solubility is a molecular property decisive in the entire process from the drug development and design to the final drug formulation and production, the main objective of this paper is ~~explaining~~ to explainthe effect of the variance in molecular properties and intermolecular interaction on dissolution by Hansen Solubility Parameter (HSP) and KAT-LSER model.
Place and Duration of Study: Department of Biomedical Sciences, Faculty of Pharmacy. Between April 2023-April 2024.
Methodology: The solubility of the drug was measured in pure monosolvents of several chemical classes keys in formulation, purification, and crystal formation of drugs. HSP was tested to determine the partial solubility parameters of caffeine. The logarithm of the mole fraction experimental solubility ln*X*2 as the dependent variable was used. KAT-LSER model was used to show that solute-solvent interactions are principally attributed to the dipolarity/polarizability interaction and the hydrogen bonding basicity. Differential scanning calorimetry (DSC) and Fourier transform infrared spectroscopy (FT-IR) were performed for the original powder and ~~for~~ the solid phase after equilibration with the pure solvents.
Results: Good results were obtained with the model of three- and four- partial parameters of solubility. Since the dispersion parameter does not greatly vary from one drug to another, the variation of solubility among solvents is largely due to the dipolar and hydrogen bonding parameters, a fact that is ~~being~~ consistently found for other drugs of small molecular weight. DSC and FT-IR allow ~~detecting~~ detectionof possible changes ~~of~~ inthe thermal properties of the solid phase and verify the anhydrous nature of the starting material.
Conclusion: The results showed that the solubility of caffeine is mostly affected by polarity and/or hydrogen bonding.

Keywords: Hansen Solubility Parameter, caffeine, characterization, Expanded Hansen Method, KAT-LSER model.

1. INTRODUCTION

Caffeine (3,7-Dihydro-1,3,7-trimethyl-1H-purine-2,6-dione) (CAS 58-08-2, molecular formula $C_8H_{10}N_4O_2$ and molar mass 194.19 g·mol^{-1}) is a methylxanthine alkaloid structurally related

to adenosine and acts primarily as an adenosine receptor antagonist with psychotropic and anti-inflammatory activities (**Fig. 1**). Upon ingestion, caffeine binds to adenosine receptors in the central nervous system, which inhibits adenosine binding. This inhibits the adenosine-mediated downregulation of central nervous system activity; thus, stimulating the activity of the medullary, vagal, vasomotor, and respiratory centers in the brain. This agent also promotes neurotransmitter release that further stimulates the central nervous system. The anti-inflammatory effects of caffeine are due to the nonselective competitive inhibition of phosphodiesterases. Inhibition of Cyclic Nucleotide Phosphodiesterases (PDEs) raises the intracellular concentration of cyclic AMP (cAMP), activates protein kinase A, and inhibits leukotriene synthesis, which leads to reduced inflammation and innate immunity.

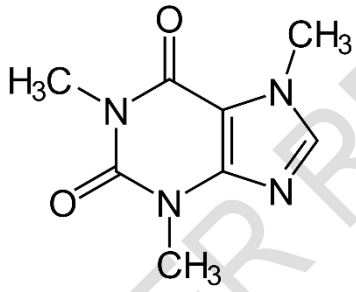

Fig. 1. Chemical structure of caffeine

The physical and chemical properties of drugs are of great importance for ~~the~~ production and industrial application, and among them, solubility is crucial for the crystallization and purification process to produce high quality, stable and large-scale drugs. Starting from this base, the solid-liquid balance of caffeine in several pure solvents has been studied to improve the industrial production processes of formulations with this drug[1, 2]. The Hansen Solubility Parameter (HSP) is a powerful tool for evaluating the solute dissolution process.

The cohesive energy density, represented by the square of the solubility parameter (δ), was decomposed into contributions stemming from nonpolar interactions (van der Waals dispersion forces), dipole interactions, and hydrogen bonding [3-5]:

$$\delta_T^2 = \Delta E/\Delta V = \frac{\Delta E}{V} = \frac{\Delta E_d}{V} + \frac{\Delta E_p}{V} + \frac{\Delta E_h}{V} \qquad (1)$$

where, ΔE, is the vaporization energy of the compound; the terms δ_d, δ_p, and δ_h denote partial parameters that respectively represent the dispersion, polar, and hydrogen bonding components of the overall solubility parameter, δ_T. Additionally, ΔV stands for the molar volume of the compound.

Later, Karger et al. [6] improved the original scheme of Hansen by dividing the hydrogen bonding parameter, δ_h into a proton donor or Lewis acid term δ_a and a proton acceptor or Lewis base term δ_b, due to hydrogen bonding was used in Eq. (1) in a general sense, to mean highly polar oriented interactions of specific donor-acceptor types. Bustamante et al. [7-11] found that it is possible to directly regress ln X_2 against the three- or four- partial solubility parameters. The modified models are:

$$ln\ X_2 = C_o + C_1\delta_{1d}^2 + C_2\delta_{1d} + C_3\delta_{1p}^2 + C_4\delta_{1p} + C_5\delta_{1h}^2 + C_6\delta_{1h} \quad (2)$$

and

$$ln\ X_2 = C_o + C_1\delta_{1d}^2 + C_2\delta_{1d} + C_3\delta_{1p}^2 + C_4\delta_{1p} + C_5\delta_{1a} + C_6\delta_{1b} + C_7\delta_{1a}\delta_{1b} \quad (3)$$

Equations (2) and (3) can be employed to compute the partial solubility parameters of the solute by utilizing the ratio of the coefficients in formulations equivalent to Equations (4) and (5).

$$\delta_{2d} = -(C_2/2C_1);\ \delta_{2p} = -(C_4/2C_3) \text{ and } \delta_{2h} = -(C_6/2C_5) \quad (4)$$

$$\delta_{2d} = -(C_2/2C_1);\ \delta_{2p} = -(C_4/2C_3);\ \delta_{2a} = -(C_6/C_7) \text{ and } \delta_{2b} = -(C_5/C_7) \quad (5)$$

The solubility of caffeine, in this work, in 17 pure solvents, which belongs to different chemical classes and they are widely used in the pharmaceutical industry including manufacturing and purification, was measured at T = 298.15 K and p = 0.1 MPa. The knowledge of appropriate solvents along with their dissolution ability of crystalline compounds helps to discover the optimum number of solvent systems to practice in some definite applications. The solid-liquid equilibrium method has been utilized to calculate the solubility. Experimental solubility values are employed to test the three- and four-parameter models of the Expanded Hansen Method, aiming to evaluate the partial solubility parameters of caffeine.

To end, the solvent effect was analyzed by KAT-LSER model which indicated that the solute–solvent interactions came into prominence in the solubility of caffeine [12-17].

2. MATERIAL AND METHODS

2.1 Materials

Caffeine (mass fraction purity > 0.999) was supplied by Sigma-Aldrich (Germany). The solvents used were analytical or spectrophotometric grade. **Table 1** presents the theoretical values of the

partial solubility parameters of the pure solvents that we used in the study, dispersion, dipolar, hydrogen bonding, acid and basic in $(MPa)^{1/2}$, and the molecular weights in g/mol.

Table 1. Values of HSP of selected solvents [18]

Solvents	δ_T	δ_d	δ_p	δ_h	δ_a	δ_b	MW
Hexane	14.9	14.9	0.0	0.0	0	0	86.18
Cyclohexane	16.8	16.8	0.0	0.2	0	0	84.16
Carbitol	16.2	9.2	12.3	22.3	-	-	134.1
Isopropyl myristate	17.5	16.4	2.0	5.7	0	5.7	270.45
Carbon tetrachloride	17.8	17.8	0.0	0.6	0	1.84	153.81
Ethyl acetate	18.1	15.8	5.3	7.2	10.84	3.89	88.11
Benzene	18.6	18.4	0,0	2.0	1.43	1.4	78.11
Dichloromethane	20.3	18.2	6.3	6.1	7.1	0	84.93
1,2-Dichloroethane	20.9	19.0	7,4	4.1	4.1	2	96.95
Trichloromethane	19.0	17.8	3.1	5.7	6.1	2.7	119.37
1,4-Dioxane	20.5	19.0	1.8	7.4	2.04	13.29	88.11
Acetic acid	21.4	14.5	8,0	13.5	14.32	6.34	60.05
Propionic acid	20.7	14.7	7.8	12.3	12.27	6.14	74.08
N-methyl-2-pyrrolidone	22.9	18.0	12.3	7.2	0	7.2	99.13
Acetone	20.0	15.5	10.4	7.0	4.9	4.9	58.08
Acetophenone	21.8	19.6	8.6	3,7	2.25	3.07	120.15
Methanol	29.6	15.1	12.3	22.3	17.2	22.3	32.04
Ethanol	26.5	15.8	8.8	19.4	16.98	11.25	46.07
1-Pentanol	21.7	16.0	4,5	13,9	11.04	8,79	88.15
1-Propanol	24.5	16.0	6.8	17.4	15.3	9.8	60.10
2-Propanol	23.5	15.8	6.1	16.4	14.5	9.2	60.10
1,2-Propanediol	30.2	16.8	9.4	23.3	28.80	9.4	76.09
Ethylene glycol	32.9	17.0	11.0	26.0	36.6	9	62.07
Diethyl ether	15.8	14.5	2.9	5.1	1.0	12.9	74.12
Formamide	36.6	17.2	26.2	19.0	11.7	15.60	45.04
Dimethylformamide	24.8	17.4	13.7	11.3	6.95	9	73.10
Water	47.8	15.6	16.0	42.3	13.70	65.46	18.00

2.1 Solubility measurements

Sealed flasks, each containing a slight excess of powder dissolved in the pure solvents outlined in Table 1, were prepared, and placed in a temperature-controlled bath with constant agitation at 25 °C (± 0.1 K) (HETO® Type SBD50-1 bio. 501828H. Paris, France). The clear solutions were diluted with ethanol 96 % v/v and assayed in a double beam spectrophotometer (Agilent®

61030AX. CA. United States) at the previously selected wavelength for each drug (λ = 273 nm). None of the solvents interfered with the spectrophotometric readings. The calibration curve was prepared by plotting absorbance versus concentration of the drug, and the saturation curves in water were obtained (4 days) to estimate the conditions of agitation and time needed to attain equilibrium solubility in the solvents used. After equilibrium was attained, the non-dissolved solid phase was removed by filtration (Durapore membranes 0.2 µm pore size, Darmstadt, Germany). The densities of the solutions were measured at 25°C (± 0.1 K) using 10-mL pycnometers, facilitating the conversion of molarity units into mole fraction units. Experimental data represent the average of at least three replicated experiments. The coefficient of variation (CV), computed as the ratio of the standard deviation to the mean and expressed as a percentage, falls within 2 % among the replicated samples, with most cases exhibiting less than 1.5 % variation.

2.2 Water content determination

The water content of the original powders was analyzed in triplicate using the Karl-Fischer rapid test method [19].The solvent is placed in a glass bottle and titrated with the Karl-Fisher reactants. After having added a sample of the powder accurately weighed, the solution is again titrated, and the water content of the sample (grams) is calculated in % by ~~weigh~~ weightfrom the milliliters of titrant used.

2.3 Differential Scanning Calorimetry (DSC)

The melting point and the heat of fusion of the original powders of the drug was determined by Differential Scanning Calorimetry **(**DSC) (DSC 3, Mettler, Schwerzenbach, Switzerland). The calibration of the equipment was carried out with the metals, indium (In, purity 99.999 %) and zinc (Zn, purity 99.998 %) both standards from Mettler Toledo (Schwerzenbach, Switzerland). In addition, the thermograms of each solid phase after equilibration with the pure solvents were also obtained. The weight of the samples analyzed is comprised of over 3 mg (± 0.01 mg). A program of 30 to 300 ºC was chosen, with a heating rate of 5 ^{o}C/min. For this analysis, each solid phase was gently dried at room temperature to prevent the removal of solvent that is loosely bound to the crystals, as this may impact the thermal behavior of the solid phase [20, 21].

2.4 Hot-Stage Microscopic (HSM)

The Hot-Stage Microscopic (HSM) experiment was carried out using an Olympus BX-50 microscope connected to a HFS 91 hot stage (Shinjuku, Japan) and a temperature controller, to observe the solid phase behavior before and after equilibration with the saturated solutions under polarized light in the range of 30–300 °C at a heating rate of 5 °C/min.About 3 mg (± 0.01 mg) of the sample was positioned between two thin (0.13–0.15 mm) glass slides and put on a hot stage (Semic, Bioelektronika, Krakow, Poland).

2.5 Differential Scanning Calorimetry (DSC)

The Fourier Transform Infrared Spectroscopy (FT-IR) analysis was executed with the equipment Fourier Spectrum 2000 spectrometer Perkin Elmer System 20000FT-IR (EE.UU.) with a resolution of 1 cm^{-1}. For the analysis, a dilution of 5:95 with KBr was uniformly mixed in an agate mortar. This mixture is placed in a hydrostatic press and means of high pressure (10 T for 3 min), discs of about ~~obtain~~ 10 mm in diameter.The background spectrum was recorded prior to taking each measurement.

2.6 Statistical analysis of experimental results

The three- and four-parameter models of the Expanded Hansen Method were tested using as dependent variable, ln X_2. Robust regression methods as well as analysis of residuals were used to detect ~~inconsistences~~ inconsistencies~~of~~ between individual cases with the overall model. From these results, weighted regressions were conducted, assigning a smaller weight to the solvents that fit the model less accurately.

3. RESULTS AND DISCUSSION

3.1 Influence of the individual solvents on the solid phase of caffeine

Figure 2 illustrates the thermogram of the original caffeine powder Form II, showing the first endotherm at 153.18 ^{o}C related to the solid-solid transition from one polymorphic form to another (transition enthalpy 16.08 J/g), and a second endothermic event at 234.56 ^{o}C, that corresponds to fusion (fusion enthalpy of 119.94 J/g). This endothermic peak is due to the melting of Form II.

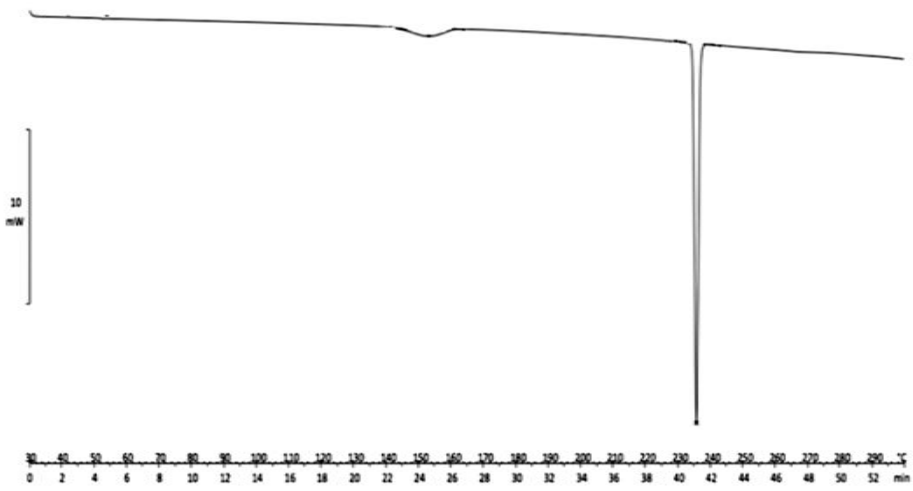

Fig. 2. DSC curve of caffeine original powder

These results agree with previous published ones, in which caffeine ~~show~~ shows two enantiotropically related anhydrous polymorphic forms, Forms I and II, and a hydrated form. This hydrate is converted to a Form II under ambient temperature and atmospheric pressure conditions which, in turn, changes enantiotropically to Form I at 155 °C. Finally, an isotropic liquid can be obtained by heating this phase at 237 °C [22]. The absorption of the hydrated form occurs about three times faster for ~~the~~ Form I than for ~~the~~ Form II, and Form I turns to the hydrate at about twice the rate of Form II [23]. Form I is the most soluble and metastable, and Form II is the least soluble but stable form [24]. The stable Form II is frequently used in the formulations of solid dosage forms and is a final product of the dehydration process [25], which becomes the Form metastable I when heated over a wide temperature range of 418–426 K [26], or pressure of about 50 MPa [27]. Some authors consider the existence of Form III [28], while, according to others, it is a separate mixture of two Forms I and II [29]. Although the Form I metastable state is long-lived, at room temperature it becomes extremely slow (weeks to months) to the Form II [30, 31].

In this work, additional techniques such as thermomicroscopy (HSM), FT-IR spectroscopy, and Karl-Fisher method were used to further corroborate this result. Caffeine may be hygroscopic; it must be preserved in the absence of humidity in hermetically closed containers. To find out the amount of moisture in the original powder, Karl-Fisher titration was performed, it was obtained a percentage of about 1-2 % water.Numerous works have been presented previously to reduce the hygroscopicity of drugs such as caffeine, flufenamic acid, or

levofloxacin and metacetamol[32-34], using cocrystal which exhibited superior stability to humidity over original drugs.

The DSC-results obtained are exposed in **Table 2**, where the melting temperature (T_{fusion}) and the molar enthalpy of melting (ΔH_{fusion}) are collected for each of the solid samples studied, any of these results are showed in **Fig. 3**.

Table 2.Results DSC of transition and fusion for caffeine in ~~monosolvents~~ mono solventsselected

Solvents	$T_{transition}$ (°C)	$\Delta H_{transition}$ (J/g)	T_{fusion}(°C)	ΔH_{fusion}(J/g)
Caffeine	153.18	16.08	234.40	119.94
Water	142.14	13.29	232.35	121.11
1,2-Propanediol	146.94	16.08	233.35	119.94
Formamide	149.71	13.39	235.14	122.59
1,2-Dichloroethane	146.70	14.13	233.98	121.39
Benzene	-	-	234,28	121.39
Isopropyl myristate	142.35	6.75	226.27	112.66
1-Pentanol	146.64	5.25	234,44	89.33
Propionic acid	139.78	13.70	234.40	128.16
Acetophenone	-	-	233.66	118.39
Acetic acid	138.73	8.09	233.69	101.81
Dimethylformamide	147.18	10.02	232.98	99.44
Ethanol	146.40	11.69	234.09	124.86
Hexane	146.81	13.30	234.98	115.69
Ethyl acetate	143.81	3.31	234.54	115.25
Cyclohexane	146.86	14.57	234.69	113.19
1,4-Dioxane	144.56	12.53	234.78	116.29
Trichloromethane	149.28	5.39	233.93	115.64

During the solubility experiments, the crystalline form of the solid phase might undergo alteration. These changes can potentially modify the heat and/or temperature of fusion of the solid phases, resulting in ideal solubility values that differ from the value determined for the original powder. Along with this, it should be emphasized that the endothermic peak, due to the phase transition of Form II to Form I, can be modified, as can be seen in **Table 2**. The DSC anhydrous caffeine showed a similar thermal behavior except for benzene and acetophenone

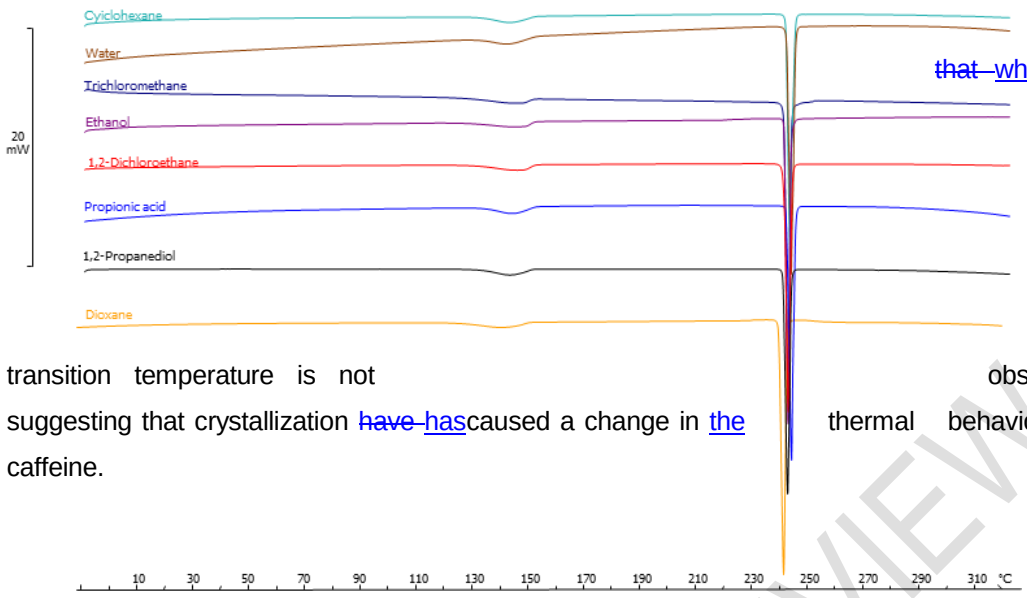

~~that~~ where the phase transition temperature is not observed, suggesting that crystallization ~~have~~ has caused a change in the thermal behavior of caffeine.

Fig. 3. DSC solid phases of caffeine in any ~~monosolvents~~mono solvents

HSM is an analytical technique that combines microscopy with thermal analysis~~,~~ and has been used to characterize the solid phases obtained as a function of time and temperature. The thermal behavior observed by HSM analysis confirmed the DSC results, obtaining a temperature of fusion at 241 ºC, to the same heating rate (5 ºC/min), allowing moreover visualizing changes in the crystal and confirming the transitions and the absence of hydrates.

On the other hand, the FT-IR spectra of the original caffeine powder and ~~of~~ each solid excess in contact with the pure solvents used are shown in **Figures 4** and **5**, the most significant peaks of the original caffeine powder appear marked.The spectrum of caffeine shows two relatively strong bands located at 1705 and 1659 cm^{-1} that originate from the stretch vibrations of the carbonyl groups and around 1600 cm^{-1} for the group, C=C-.With all the solvents a similar behavior was observed in terms of the infrared spectrum of caffeine.

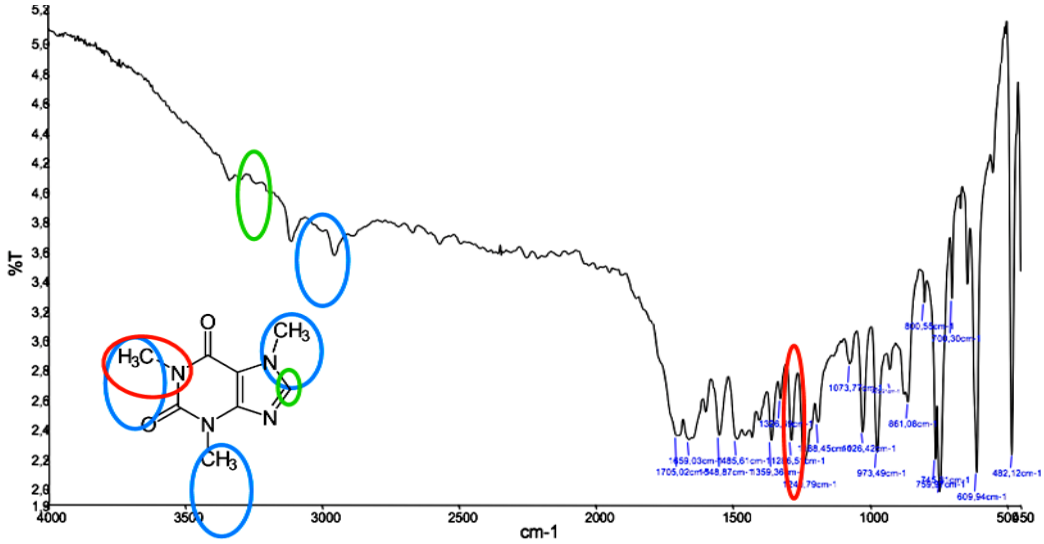

Fig. 4. FT-IR caffeine spectrum original powder

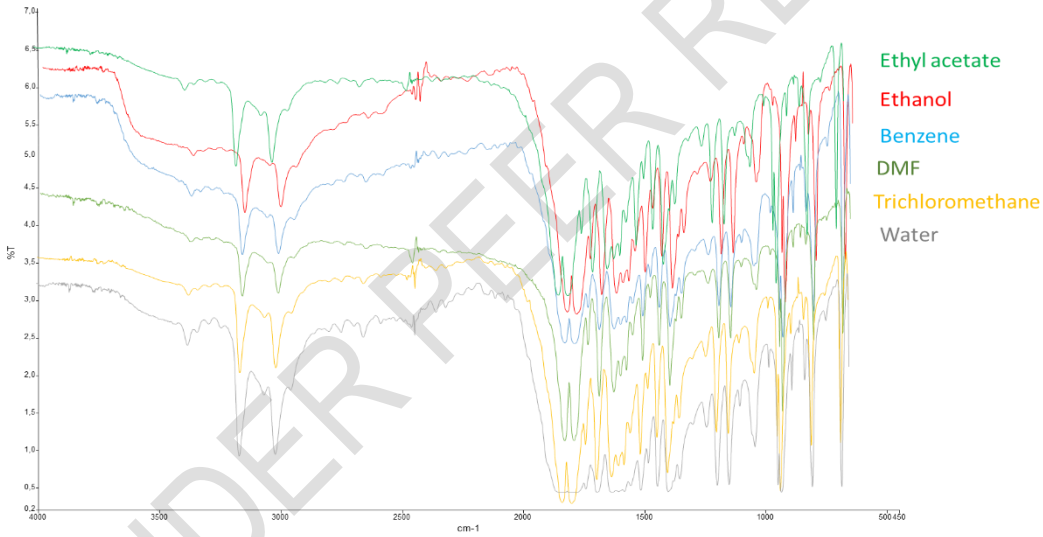

Fig. 5. FT-IR caffeine in any ~~monosolvents~~mono solvents

3.2Partial solubility parameters of caffeine

Table 3 and **Figure 6**~~includes~~ includethe experimental logarithm of the mole fraction solubility (ln X_2) of caffeine against the total solubility parameter of the 17 particular solvents selected, at 298 K. The solubility of caffeine was the highest in formamide and the lowest in non-polar solvents, hexane, and cyclohexane. According to the experimental results, the solvents with better solubility were selected as co-solvents, and the solvents with poor solubility ~~was~~ wereselected as the anti-solvent. The parameters are calculated from coefficients that are significant at least at the 0.05 probability level. A weight of 0.01 was assigned to some

~~solvent~~solvents, which least fit the three- model, and ~~for~~ the four- model. For the remaining solvents, the weight was fixed at unity, in both cases.

Table 3.Experimental solubility (X_2) of caffeine

Solvents	Volume		X_2	ln X_2
Hexane		131.6	2.50E-05	-10.597
Diethyl ether [35]		104.8	1.15E-03	-6.770
Carbitol[36]		130.9	7.62E-03	-4.877
Cyclohexane		108.7	2.09E-05	-10,776
Isopropyl myristate		318.2	2.00E-03	-6.215
Carbon tetrachloride [37]		97.1	1.56E-03	-6.461
Ethyl acetate		98.5	1.05E-02	-4.556
Benzene		89.4	5.10E-03	-5.279
Trichloromethane		80.7	4.80E-02	-3.037
Acetone [37]		74.0	4.54E-03	-5.396
Dichloromethane [37]		63.9	3.70E-02	-3.298
1,4-Dioxane		85.7	8.20E-03	-4.804
Propionic acid		75.0	7.10E-03	-4.948
1,2-Dichloroethane		79.4	3.07E-01	-1.181
Acetic acid		57.1	2.66E-01	-1.324
1-Pentanol		109.0	3.70E-03	-5.599
Acetophenone		117.4	4.27E-01	-0.851
N-methyl-2-pyrrolidone [38]		96.5	1.49E-02	-4.206
1-Propanol [38]		75.2	1.78E-03	-6.331
2-Propanol [39]		76.8	1.70E-03	-6.377
Dimethylformamide		77.0	1.85E-02	-3.990
Ethanol		58.5	2.70E-03	-5.915
Methanol [40]		40.7	2.55E-03	-5.972
1,2-Propanediol		73.6	2.06E-02	-3.882
Ethylene glicol [41]		55.8	3.17E-03	-5.754
Formamide		39.8	6.00E-01	-0.511
Water		18.0	2.20E-03	-6.119

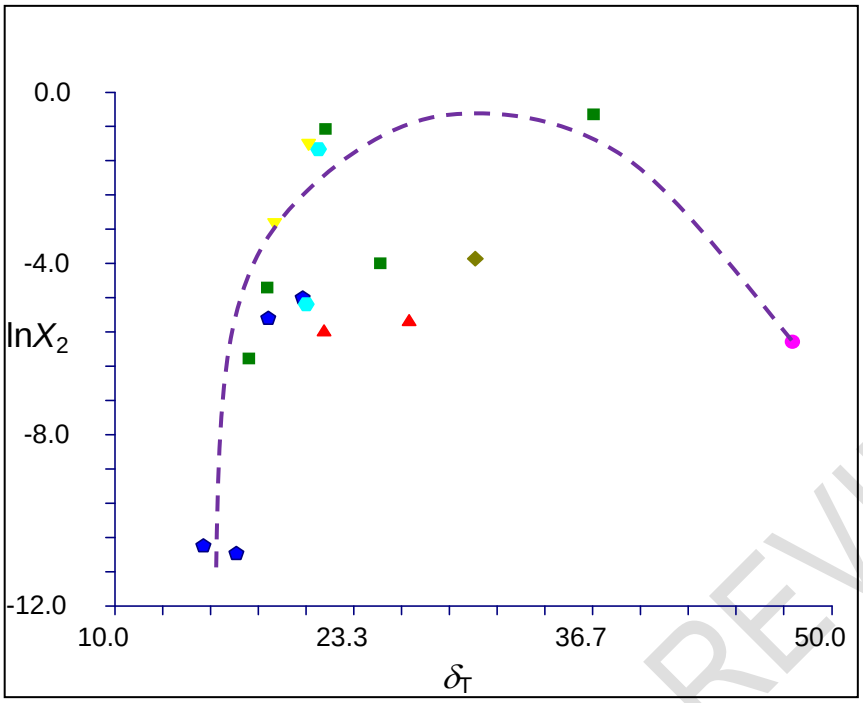

Fig. 6. Experimental logarithm of the mole fraction solubility of caffeine against the total solubility parameter in water (●), non-polar (●), bases (■), acids (●), alcohols (▲), halogenated (▼) and glycols (◆) solvents

Three- and four- parameter models did provide significant t-values for all the coefficients. The partial solubility parameters obtained with the dependent variable ln X_2 were obtained from the regression coefficients (**Table 4**).

Table 4 Partial solubility parameters of caffeine using lnX_2 as dependent ~~variable~~[a]variable

Models	δ_d	δ_p	δ_h	δ_a	δ_b	δ_T	r^2
Three-	12.52	28.75	13.50	-	-	$\delta^2_T = \delta^2_d + \delta^2_p + \delta^2_h = 34.11$	0.80
Four-	11.62	28.52	12.30	7.64	9.91	$\delta^2_T = \delta^2_d + \delta^2_p + 2\delta_a\,\delta_b = 33.16$	0.95

[a] The values are given in the SI system ($MPa^{1/2}$).

Total solubility parameter of the caffeine was calculated for other investigators, Bustamante et al. [42] have also proposed a value for the total solubility parameter but was calculated in solvent mixtures, water-ethanol, and ethanol-ethyl acetate, (δ_T = 26.51 and 20.0 $MPa^{1/2}$) or using Hoy method was obtained a value of 27.48 $MPa^{1/2}$ [43].

The values of δ_d are correct, in fact, it is known that the dispersion parameter varies in the value scale around 12 $MPa^{1/2}$ because it is the interval where most of the values of the solvent parameters are included pure. One accepted explanation is that it represents the London dispersion forces, an interaction applicable to both polar and nonpolar molecules. Therefore, the rest of the parameters are the most useful to determine the behavior of drugs, in relation to their solubility, affinity with excipients, diffusion, or absorption through biological membranes. The hydrogen bond solubility parameter can be calculated using the experimental value of the acid and basic solubility parameters, with the following expression Eq. (6):

$$\delta^2_h = 2\ \delta_a\ \delta_b \quad (6)$$

The value of δ_h= 13 $MPa^{1/2}$ is according to other investigations [35-46]. It has been observed that the value of the partial acid and basic parameters are according to the functional groups of the molecule (**Figure 1**), the fact that δ_b is larger than δ_a is consistent with the higher solubility of caffeine in acidic solvents and with the presence of a hydrogen bond acceptor on the molecule.

In addition, the HSP values of caffeine were calculated using the contribution of each group, and their mathematical relationship is summarized below, as proposed by Hoftyzer and van Krevelen[47]. The equations for the computing of δ_d, δ_p, and δ_h are:

$$\delta_d = \frac{\sum nF_d}{\sum nV} \quad (7)$$

$$\delta_p = \frac{\sqrt{\sum nF_p^2}}{\sum nV} \quad (8)$$

$$\delta_h = \sqrt{\frac{\sum nF_d}{\sum nV}} \quad (9)$$

where *F*d represents the contribution to the dispersion force; *F*p stands for the contribution to the polarity force; and *U*h stands for the contribution to the hydrogen bond interaction energy.

The molar volume (ΔV) (130.2 cm^3/mol) ~~have~~ has been calculated with the Fedors group-contribution method [48, 49] (**Table 5**). The values of *F*d, *F*p, and *U*h for each group of caffeine structure as well as the HSP are collected in **Table 6**.

Table 5.Fedors method to estimate the internal energy (Δ*E*), molar volume (Δ*V*), and Hildebrand solubility parameter of caffeine

Group or atom	n_i	Δ*E*(kJ/mol)	Δ*V*(cm^3/mol)
($-CH_3$)	3	14.13	100.5
(>CH=)	1	4.31	13.5
(-C=)	2	8.62	- 11.0
Ring closure > atoms	2	2.1	32.0
Conjugated double bond in a closed ring	2	3.34	- 4.4
(>C=O)	2	34.8	21.6
(-N<)	1	12.6	- 27.0
(N=)	3	11.7	5.0

$$\delta_2 = (\sum E / \sum V)^{1/2} = 26.52 \text{ MPa}^{1/2}$$

Table 6.Application of the Hoftyzer–van ~~Krevelen'~~ Krevelen method to estimate the partial solubility parameter of caffeine

Group or atom	n_i	n_iF_di	$(n_iF_pi)^2$	n_iU_{hi}
CH_3	3	1260	0	0
(>CH=)	1	200	0	0
(-C=)	2	70	0	0
(>C=O)	2	290	770	2000
(-N<)	1	160	210	3100
N=	3	20	640000	5000
NH	1	160	44100	3100

$\delta_d = (\sum n_i F_{di}) / V$ **20.28 MPa^{½}**

$\delta_p = (\sqrt{(\sum n_i F_p i)^2}) / V$ **22.75 MPa^{½}**

$\delta_h = (\sqrt{(\sum n_i U_{hi})} / V)$ **13.58 MPa^{½}**

$$\delta_T = \sqrt{\left[(\delta_d)^2 + (\delta_p)^2 + (\delta_h)^2\right]}$$ **33.36 MPa^{½}**

3.3Solvent effects: KAT-LSER model

The KAT-LSER (Kamlet-Abboud-Taft linear solvation energy relationship) model is working to analyse the solubility of caffeine, aiming to elucidate the effects of Lewis acid-base interactions and polarization on the enhancement of this property. Classical KAT-LSER model takes the form of Eq. (10) [50, 51].

$$\ln x_2 = c_0 + c_1\alpha + c_2\beta + c_3\pi + c_4\left(\frac{V_2\delta_1^2}{100RT}\right) \quad (10)$$

where, $c_1\alpha$ and $c_2\beta$ refer to the energy terms for specific solute–solvent Lewis acid and base interactions, respectively; $c_3\pi$ represents the energy term for non-specific interactions; whereas, the last term in ~~the~~ Eq. (10) denotes the cavity term defining the energy for solvent–solvent molecule interactions. This term describes the drug accommodation energy as a product of the HSP, and molar volume of caffeine, V_2.

The universal gas constant, R, and the experimental temperature, T/K, are included in the denominator to obtain a ~~dimension less~~dimensionless magnitude of the cavity term. c_0 symbolizes the solute-solute interactions and measures the intercept when $\alpha=\beta=\pi=\delta_2=0$; c_1 and c_2 gauge the property susceptibility of caffeine to specific solute-solvent interactions, particularly hydrogen bonding, whereas c_3 and c_4 represent the solute's sensitivity to nonspecific electrostatic solute-solvent and solvent-solvent molecule interactions. **Table 7** summarizes the solvatochromic parameters α, β, and π, as well as the HSP of solvents studied in this research~~,~~ gathered from the literature [52].

Table 7.Solvatochromic parameters and total HSP of some ~~solvent~~ solvents studied [50]

Solvents	α^a	β^a	π^a	δ_2 **(MPa$^{1/2}$)** ^{b}
Hexane	14.9	0.00	0.00	-0.11
Diethylether	15.8	0.00	0.47	0.24
Cyclohexane	16.8	0.00	0.00	0.00
Carbontetrachloride	17.8	0.00	0.10	0.21
Ethylacetate	18.1	0.00	0.45	0.45
Benzene	18.6	0.00	0.10	0.55
Trichloromethane	19.0	0.20	0.10	0.58
Acetone	20.0	0.08	0.48	0.62
Dichloromethane	20.3	0.13	0.10	0.82
Dioxane	20.5	0.00	0.37	0.49
Propionicacid	20.7	1.12	0.45	0.58

1,2-Dichloroethane	20.9	0.00	0.10	0.73
Aceticacid	21.4	1.12	0.45	0.64
1-Pentanol	21.7	0.84	0.86	0.40
Acetophenone	21.8	0.04	0.49	0.81
NMP	22.9	0.00	0.77	0.92
2-Propanol	23.5	0.76	0.84	0.48
1-Propanol	24.5	0.84	0.90	0.52
Dimethylformamide	24.8	0.00	0.69	0.88
Ethanol	26.5	0.86	0.75	0.54
Methanol	29.6	0.98	0.66	0.60
1,2-Propanediol	30.2	0.83	0.78	0.76
Ethyleneglycol	32.9	0.90	0.52	0.92
Formamide	36.6	0.71	0.48	0.97
Water	47.8	1.17	0.47	1.09

[a] Taken from Marcus [53]. [b] Taken from Barton [18].

In this way, KAT-LSER model obtained is presented as Eq. (11) (r = 0.84 and *F* = 11.42).

$$\ln X_2 = -8.14 + 1.05\alpha - 1{,}67\,\beta + 9.76\,\pi - 7.06\left(\frac{V_2\delta_1^2}{100\,RT}\right) \qquad (11)$$

Positive values of c_1 (1.05), and c_3 (9.76) demonstrate the favourable contribution of Lewis-acid base and polarizability of caffeine solubility, whereas the negative values of c_0 (-8.14), c_2 (-1.67) and c_4 (-7.06) demonstrate the unfavourable contribution of solute-solute interactions and cavity energy requirements on the solubility of this drug. Moreover, if absolute values of c_1, c_2, c_3 and c_4 are compared the following contribution % are attained: 5.37, 8.55, 49.95 and 36.13 %, respectively, which means that polarization effects imply the higher contribution ~~on~~ of solubilisation, followed by the Lewis acid behaviour of caffeine owingprobably the hydrogen atom of the heterocycle secondary amine group [54].

4. CONCLUSION

In this work, the solid–liquid equilibrium solubility of caffeine in different 17 mono-solvents belongs several chemical classes was studied by shake-flask technique at 298.15 K. Studying the solid-liquid phase equilibrium and Hansen Solubility Parameters (HSP) of caffeine is crucial for achieving better online control and in-time optimization in the industrial crystallization process, ultimately leading to the production of high-quality crystal

products.This comprehensive approach enables a better understanding of the relationship between molecular properties, solvent characteristics, and caffeine solubility, ultimately contributing to the optimization of industrial processes involving caffeine crystallization and dissolution.

In this paper, the focus lies on elucidating the role of molecular properties and intermolecular interactions in drug dissolution, particularly through the lens of the Hansen Solubility Parameters (HSP) and the KAT-LSER model. The KAT-LSER model, a powerful tool, is utilized to quantify the influence of various intermolecular interactions on the dissolution process of caffeine. By employing this model, researchers can investigate how different types of intermolecular forces impact the solubility of caffeine, paying particular attention to polarization effects. This approach allows for a more comprehensive understanding of the dissolution behavior of caffeine, shedding light on critical factors that influence its solubility in different environments.

Partial solubility parameters were obtained by the Bustamante et al. method from experimental solubility values, obtaining the values, δ_T = 34.11 $MPa^{1/2}$ and δ_T = 32.16 $MPa^{1/2}$, using the three- and four- parameter models. Then, the Total Hildebrand solubility parameter was calculated based on group contributions using the Fedors and Hoftyzer-van Krevelen methods, resulting in values of 26.52 and 33.36 $MPa^{1/2}$, respectively.These calculations offer a comprehensive understanding of the overall solubility characteristics of caffeine, considering the combined effects of various molecular groups and interactions.

REFERENCES

1. Gonçalve, L K S, Viera J B, Silva N S R, Santos C F, Braga F S, Costa J S, Macêdo W J C, Silva C H T P, Hage-Melim L I S, Santos C B R A QSAR study of new caffeine derivatives with epithelial anticancer activity. J Pharm Res Int. 2015;7(2):122–139. https://doi: 10.9734/BJPR/2015/17914.
2. Gamal M W, Ali N R, Elghobashy M, Abdelkawy M. Simultaneous determination of a ternary mixture of aspirin, caffeine and orphenadrine citrate by simple RP-TLC spectrodensitometric method. J Pharm Res Int. 2017;14(4):1–11. https://doi: 10.9734/BJPR/2016/31194.
3. Hansen CM. The three dimensional solubility parameter—key to paint component affinities I—solvents, plasticizers, polymers, and resins. J Paint Technol. 1967;39:104-117.

4. Hansen C, Beerbower A. Solubility parameters. In: encyclopedia of chemical technology, Suppl. 2nd ed., Wiley, New York, NY, 1971, pp. 896-910.
5. Hansen CM. Hansen solubility parameters. A user's Handbook, CRC Press, Boca Raton, FL. 2007.
6. Karger BL, Snyder LR, Eon C. An expanded solubility parameter treatment for classification and use of chromatographic solvents and adsorbents: Parameters for dispersion, dipole and hydrogen bonding interactions. J Chromatography. 1976;125(1):71-88. https://doi.org/10.1016/S0021-9673(00)93812-3.
7. Bustamante P, Hinkley DV, Martin A, Shi S. Statistical analysis of the extended Hansen method using the bootstrap technique. J Pharm Sci. 1991;80:971-977. https://doi.org/10.1002/jps.2600801014.
8. Bustamante P, Martin A, González-Guisandez MA. Partial solubility parameters and solvatochromic parameters for predicting the solubility of single and multiple drugs in individual solvents. J Pharm Sci. 1993;82:635-640.https/doi.org/10.1002/jps.2600820618.
9. Bustamante P, Peña MA, Barra J. Partial-solubility parameters of naproxen and sodium diclofenac. J Pharm Pharmacol. 1998;50(9):975-982. https/doi.org/10.1111/j.2042-7158.1998.tb06911.x.
10. Bustamante P, Peña MA, Barra J. Partial solubility parameters of piroxicam and niflumic acid. Int J Pharm. 1998;174:141-150. https/doi.org/10.1016/S0378-5173(98)00263-4.
11. Bustamante P, Peña MA, Barra J. The modified extended Hansen method to determine partial solubility parameters of drugs containing a single hydrogen bonding group and their sodium derivatives: benzoic acid/Na and ibuprofen/Na. Int J Pharm. 2000;194:117-124. https://doi.org/10.1016/S0378-5173(99)00374-9.
12. Li W, Qi S, Wang N, Fei Z, Farajtabar A, Zhao H. Solute-solvent and solvent-solvent interactions and preferential solvation of limonin in aqueous co-solvent mixtures of methanol and acetone. J Mol Liq. 2018;263:357-365. https://doi.org/10.1016/j.molliq.2018.05.021.
13. Li X, Liu Y, Cao Y, Cong Y, Farajtabar A, Zhao H. Solubility modeling, solvent effect, and preferential solvation of thiamphenicol in cosolvent mixtures of methanol, ethanol, N,N-dimethylformamide, and 1,4-dioxane with water. J Chem Eng Data. 2018; 63(6):2219-2227. https://doi.org/10.1021/acs.jced.8b00179.
14. Li WX, Farajtabar A, Wang N, Liu ZT, Fei ZH, Zhao HK. Solubility of chloroxine in aqueous co-solvent mixtures of N, N-dimethylformamide, dimethyl sulfoxide, N-methyl-2-pyrrolidone and 1,4-dioxane: determination, solvent effect and preferential solvation

analysis. J Chem Thermodyn. 2019;138:288-96. https://doi.org/10.1016/j.jct.2019.07.001.

15. Li Y, Li C, Gao X, Lv H. Equilibrium solubility, preferential solvation and solvent effect study of clotrimazole in several aqueous co-solvent solutions. J Chem Thermodyn. 2020;151:106255.
16. Cong Y, Du C, Xing K, Bian Y, Li X, Wang M. Investigation on co-solvency, solvent effect, Hansen solubility parameter and preferential solvation of fenbufen dissolution and models correlation. J Mol Liq. 2022;348:118415. https://doi.org/10.1016/j.molliq.2021.118415.
17. Choi E, Heynderickx PM. Solubility measurement and correlation of 2-aminoterephthalic acid in eight alcoholic solvents at different temperatures. J Chem Thermodyn. 2023;177:106948. https://doi.org/10.1016/j.jct.2022.106948.
18. Barton AFM. Handbook of solubility parameters and other cohesion parameters, 2nd ed., CRC Press, Boca Raton, FL. 1991.
19. Medvedevskikh MY, Sergeeva AS, Shokhina OS, Krasheninina MP. Features of the development of reference materials of pharmaceutical substances. Measurement Techniques. 2022;65(9):686-694. https://doi.org/10.1007/s11018-023-02140-w.
20. Rubino JT, Yalkowsky SH.Cosolvency and deviations from log-linear solubilization. Pharm Res. 1987;4:231-236. https://doi.org/10.1023/A:1016408211963.
21. Wünsche S, Yuan L, Seidel-Morgenstern A, Lorenz H. 2 A contribution to the solid state forms of bis(demethoxy)curcumin: Co-crystal screening and characterization. Molecules. 2021;26(3):720 (2021). https://doi.org/10.3390/molecules26030720.
22. Pinto SS, Diogo HP Thermochemical study of two anhydrous polymorphs of caffeine. J Chem Thermodyn. 2006;38:1515–1522. https://doi.org/10.1016/j.jct.2006.04.008.
23. Pirttimäki J, Laine E. The transformation of anhydrate and hydrate forms of caffeine at 100% RH and 0% RH. Eur J Pharm Sci. 1994;1(4):203-208. https://doi.org/10.1016/0928-0987(94)90005-1.
24. Mazel V, Delplace C, Busignies V, Faivre V, Tchoreloff P, Yagoubi N. Polymorphic transformation of anhydrous caffeine under compression and grinding: a re-evaluation. Drug Dev Ind Pharm. 2011;37(7):832-840. https://doi.org/10.3109/03639045.2010.545416.
25. Griesser UJ, Szelagiewicz M, Hofmeier UC, Pitt C, Cianferani S. Vapor pressure and heat of sublimation of crystal polymorphs. J Therm Anal Calorim. 1888;57:45-60. https://doi.org/10.1023/A:1010188923713.
26. Matsuo K, Matsuoka M. Kinetics of solid state polymorphic transition of caffeine. J Chem Eng Jpn. 2007; 40:468-472 (2007). https://doi.org/10.1252/jcej.40.468.

27. Hubert S, Briancon S, Hedoux A, Guinet Y, Paccou L, Fessi H, Puel F. Process induced transformations during tablet manufacturing: Phase transition analysis of caffeine using DSC and low frequency micro-Raman spectroscopy. Int J Pharm, 2011;420:76-83 (2011). https://doi.org/10.1016/j.ijpharm.2011.08.028.
28. Descamps M, Decroix AA. Polymorphism and disorder in caffeine: Dielectric investigation of molecular mobilities. J Mol Struct. 2014;1078:165-173. https://doi.org/10.1016/j.molstruc.2014.04.042.
29. Enright GD, Terskikh VV, Brouwer DH, Ripmeester JA. The structure of two anhydrous polymorphs of caffeine from single-crystal diffraction and ultrahigh-field solid-state 13C NMR Spectroscopy. Cryst Growth Des. 2007;7:1406-1410 (2007).
30. Kishi Y, Matsuoka M. Phenomena and kinetics of solid-state polymorphic transition of caffeine. Cryst Growth Des. 2010;10:2916-2920. https://doi.org/10.1021/cg901405h.
31. Seliger J, Žagar V, Apih T, Gregorovič A, Latosińska M, Olejniczak GA, Latosińska JN. Polymorphism and disorder in natural active ingredients. Low and high-temperature phases of anhydrous caffeine: Spectroscopic (1H–14N NMR–NQR/14N NQR) and solid-state computational modelling (DFT/QTAIM/RDS) study. Eur J Pharm Sci, 2016;85:18-30. https://doi.org/10.1016/j.ejps.2016.01.025.
32. Aher S, Dhumal R, Mahadik K, Ketolainen J, Paradkar K. Effect of cocrystallization techniques on compressional properties of caffeine/oxalic acid 2:1 cocrystal. Pharm Dev Technol. 2013;18:55–60. https/doi.org/10.3109/10837450.2011.618950.
33. Aitipamula S, Wong ABH, Chow PS, Tan RBH.Cocrystallization with flufenamic acid: comparison of physicochemical properties of two pharmaceutical cocrystals. CrystEngComm. 2014;16: 5793–5801. https/doi.org/10.1039/C3CE42182A.
34. Shinozaki T, Ono M, Higashi K, Moribe K. A novel drug-drug cocrystal of levofloxacin and metacetamol: Reduced hygroscopicity and improved photostability of levofloxacin. J Pharm Sci . 2019;108:2383–2390. https://doi.org/10.1016/j.xphs.2019.02.014.
35. Vuong QV, Roach PD. Caffeine in green tea: Its removal and isolation. SeparatPurif Rev. 2014;43:155–174. https://doi.org/10.1080/15422119.2013.771127.
36. Rezaei H, Rahimpour E, Martinez F, Jouyban A. Solubility of caffeine in carbitol + ethanol mixture at different temperatures. J Mol Liq. 2020;301:112465. https://doi.org/10.1016/j.molliq.2020.112465.
37. Shalmashi A, Golmohammad F. Solubility of caffeine in water, ethyl acetate, ethanol, carbon tetrachloride, methanol, chloroform, dichloromethane, and acetone between 298 and 323 K. Lat Am Appl Res. 2010;40:283-285.
38. Rezaei H, Jouyban A, Zhao H, Martinez F, Rahimpour E. Solubility of caffeine in N-methyl-2-pyrrolidone + 1-propanol mixtures at different temperatures. J Mol Liq.

2022;346:117067. https://doi.org/10.1016/j.molliq.2021.116519.

39. Rezaei H, Rahimpour E, Zhao H, Martinez F, Jouyban A. Solubility measurement and thermodynamic modeling of caffeine in N-methyl-2-pyrrolidone + isopropanol mixtures at different temperatures. J Mol Liq. 2021;336:116519.
40. Cárdenas ZJ, Jiménez DM, Almanza OA, Jouyban A, Martínez F, Acree WE Jr. Solubility and preferential solvation of caffeine and theophylline in {methanol + water} mixtures at 298.15 K. J Solution Chem. 2017;46(8):1605-1624. https://doi.org/10.1007/s10953-017-0666-z.
41. Rezaei H, Rahimpour E, Martinez F, Zhao H, JouybanA.Study and mathematical modeling of caffeine solubility in N-methyl-2-pyrrolidone + ethylene glycol mixture at different temperatures. J Mol Liq. 2021;341:117350. https://doi.org/10.1016/j.molliq.2021.117067.
42. Bustamante P, Navarro J, Romero S, Escalera B. Thermodynamic origin of the solubility profile of drugs showing one or two maxima against the polarity of aqueous and nonaqueous mixtures: Niflumic acid and caffeine. J Pharm Sci. 2002;91:874-883. https://doi.org/10.1002/jps.10076.
43. Chan SY, Qi S, Craig DQM. An investigation into the influence of drug–polymer interactions on the miscibility, processability and structure of polyvinylpyrrolidone-based hot melt extrusion formulations. Int J Pharm. 2015;496(1):95-106. https://doi.org/10.1016/j.ijpharm.2015.09.063.
44. Rezaei H, Rahimpour E, Ghafourian T, Martinez F, Barzegar-Jalali M, Jouyban A. Solubility of caffeine in N-methyl-2-pyrrolidone + ethanol mixture at different temperatures. J Mol Liq. 2020;300:112354. https://doi.org/10.1016/j.molliq.2019.112354.
45. Tupe SA, Khandagale SP, Jadhav AB.Pharmaceutical cocrystals: an emerging approach to modulate physicochemical properties of active pharmaceutical ingredients. JDDT. 2023;3(4):101-112. https://doi.org/10.22270/jddt.v13i4.6016.
46. Rezaei H, Rahimpour E, Zhao H, Martinez F, Jouyban A. Determination and modeling of caffeine solubility in N-methyl-2-pyrrolidone + propylene glycol mixtures. J Mol Liq. 2021;43:117613. https://doi.org/10.1016/j.molliq.2021.117613.
47. Van Krevelen DW,Nijenhuis KT. Properties of polymers, 4th ed. Elsevier, Amsterdam. 2009.
48. Fedors RF.A method for estimating both the solubility parameters and molar volumes of liquids. Polym Eng Sci. 1974;14(2):147-154.
49. Bogardus JB. Crystalline anhydrous–hydrate phase changes of caffeine and theophylline in solvent–water mixtures. J Pharm Sci. 1983;72:837-838.

https/doi.org/10.1002/jps.2600720737.

50. Huixiang Z, Yang Z, Fumin X, Hui C, Zhenguo G, Shichao D, Yan W. Insight into the dissolution behavior of valsartan (form E) in twelve pure solvents: Solubility, modelling and molecular simulation. J Mol Liq. 2024;402:124774. https://doi.org/10.1016/j.molliq.2024.124774.
51. Munoz E, Bucchianico D, Devouge-Boyer C, Legros J, Held C, Buvat J, Moreno V,Leveneur S. Combination of linear solvation energy and linear free-energy relationships to aid the prediction of reaction kinetics: Application to the solvolysis of 5-HMF by alcohol to levulinate. Chem Eng Res Design. 2024;205:312-323. https://doi.org/10.1016/j.cherd.2024.03.040.
52. Gumireddy A, Bookwala M, Zhou D, Wildfong PLD, Buckner IS. Investigating and comparing the applicability of the R3m molecular descriptor and solubility parameter estimation approaches in predicting dispersion formation potential of APIs in a random co-polymer polyvinylpyrrolidone vinyl acetate and its homopolymer. J Pharm Sci. 2023;112(1):318-27.https/doi.org/10.1016/j.xphs.2022.11.004.
53. Marcus Y. The properties of solvents. John Wiley & Sons, Chichester. 1998. https://doi.org/10.1016/j.jct.2020.106255.
54. Marcus. Ionic liquid properties from molten salts to RTILs. Springer, 2016.